

See discussions, stats, and author profiles for this publication at: <https://www.researchgate.net/publication/271131135>

Structure–activity relationships studies of quinoxalinone derivatives as aldose reductase inhibitors

ARTICLE *in* EUROPEAN JOURNAL OF MEDICINAL CHEMISTRY · APRIL 2014

Impact Factor: 3.45

READS

12

1 AUTHOR:



[Saghir Hussain](#)

Bahauddin Zakariya University

17 PUBLICATIONS 79 CITATIONS

SEE PROFILE



Original article

Structure–activity relationships studies of quinoxalinone derivatives as aldose reductase inhibitors



Saghir Hussain, Shagufta Parveen, Xin Hao, Shuzhen Zhang, Wei Wang, Xiangyu Qin, Yanchun Yang, Xin Chen, Shaojuan Zhu, Changjin Zhu*, Bing Ma

Department of Applied Chemistry, Beijing Institute of Technology, No. 5, Zhongguancun South Street, 100081 Beijing, China

ARTICLE INFO

Article history:

Received 5 December 2013

Received in revised form

11 April 2014

Accepted 15 April 2014

Available online 21 April 2014

Keywords:

Quinoxalinone derivatives

Aldose reductase inhibitors

Structure–activity relationships

ABSTRACT

Novel quinoxalinone derivatives were synthesized and tested for their inhibitory activity against aldose reductase. Among them, N1-acetate derivatives had significant activity in a range of IC_{50} values from low micromolar to submicromolar, and compound **15a** bearing a C3-phenethyl side chain was identified as the most potent inhibitor with an IC_{50} value of 0.143 μ M. The structure–activity studies suggested that both C3-phenethyl and C6- NO_2 groups play an important role in enhancing the activity and selectivity of the quinoxalinone based inhibitors.

© 2014 Elsevier Masson SAS. All rights reserved.

1. Introduction

Diabetes Mellitus (DM) is a complex and chronic metabolic disease characterized by hyperglycemia. This disease is very common around the world and has major effect on public health. Hyperglycemia is the condition in which significant portion of the glucose enters into polyol pathway which is considered as the primary cause of pathogenesis of long-term diabetic complications, including retinopathy, nephropathy, neuropathy and cataract [1–3]. Aldose reductase (ALR2, EC 1.1.1.21) is a member of aldo-keto reductase superfamily [4,5], which catalyzes the NADPH-dependent reduction of glucose to sorbitol in the rate determining step of polyol pathway. Subsequently, the NAD^+ -dependent sorbitol dehydrogenase oxidizes the sorbitol to fructose (Fig. 1). The over production of sorbitol, imbalance of NADPH/ $NADP^+$ and NAD^+ / $NADH$ cofactors and subsequent oxidative stress inside the cells are thought to be major causes of cellular damage that develop diabetic complications. Recently, growing studies and evidences reveal that ALR2 plays a pivotal role in the development of long-term diabetic complications. Thus inhibition of ALR2 represents

the strategy and an attractive approach to prevent and delay the progression and development of diabetic complications [6].

In past few decades, structurally different Aldose reductase inhibitors (ARIs) have been developed and some of them are represented in Fig. 2, [7–17]. Unfortunately, only few of them are advanced on clinical stages for evaluation of their potency and efficacy in the treatment of peripheral neuropathy. At present only one drug, epalrestat is available in market and used in the treatment of neuropathy in Japan [8], India [18] and China. Therefore, development of more powerful ARIs is still needed.

We have been involved in the development and identification of a suitable drug candidate for the prevention and treatment of long-term diabetic complications. Recently, we have published a series of different compounds based on aromatic thiadiazine 1,1-dioxide and quinoxalinone as novel, potent and selective ARIs [19–22].

As our ongoing efforts aimed at the discovery of more pharmacophores to further design of ARIs, we have developed a new group of quinoxalinone derivatives. Herein we report their chemistry, inhibitory potency on aldose reductase and structure–activity relationships (SAR).

2. Chemistry

The synthetic methods illustrating the preparation of starting materials 3-chloroquinoxalin-(1H)-one **5** and dichloroquinoxalin-2(1H)-one **18** have been reported previously [19]. Syntheses of target compounds **7a–d**, **8a–d**, **12**, **14a–d**, **15a–b**, **17**, **22**, and **23**

Abbreviations: ALR2, aldose reductase; ALR1, aldehyde reductase; ARIs, aldose reductase inhibitors; AKR, aldo-keto reductase; NADPH, β -nicotinamide adenine dinucleotide phosphate reduced form; HNE, hydroxynoneal; SAR, structure–activity relationships.

* Corresponding author.

E-mail addresses: zcj@bit.edu.cn, zhuchangjin@tsinghua.org.cn (C. Zhu).

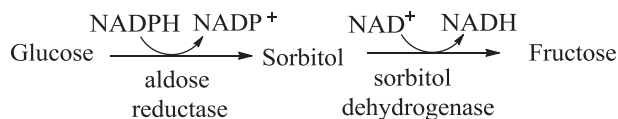


Fig. 1. The polyol pathway of glucose metabolism.

were accomplished as outlined in Schemes 1–3. As shown in Scheme 1, the 3-chloroquinoxalinone-(1*H*)-one (**5**) was *N*-alkylated with substituted *p*-nitrobenzyl bromides in the presence of K_2CO_3 producing intermediate **6**. Further reaction of **6** with various piperazines in the presence of K_2CO_3 produced the desired products **7a–d**. Alternatively, several olefines were attached, respectively, to the C3 position of compound **6** by Heck coupling reaction to obtain products **8a–c** with a vinyl linker at the C3 position, and a benzo-thiophene group was attached to the C3 position by Suzuki coupling reaction to yield **8d** [23]. Similarly, *N*-alkylation of **5** with 2-bromoacetate produced key intermediate **9**, which in turn led to a variety of products **12**, and **17**, **14a–d** and **15a–b**. The intermediate **9** was aminated with 2,4-difluoroaniline followed by nitration with mixture of $\text{Cu}(\text{NO}_3)_2 \cdot 3\text{H}_2\text{O}$ and Ac_2O [24], and then by treatment with LiOH to give **12** as shown in Scheme 2. Direct coupling of **9** with olefines led to **13a–c** and then **14a–c**, which having C3 vinyl linker, and further Pd/C catalytic hydrogenation reaction by using on the C3 double bond and the vinyl linker of **14a–b** resulted in the formation of **15a–b**. Amination of **9** with 1-(4-methoxyphenyl) piperazine produced **13d** and then **14d**. Separately, **13b** was nitrated by the same way as that for the preparation of **11** to install a nitro group at the C6 position producing **16** and **17**. Products **22** and **23** having a chloro-substituent at C6 or C7 position of the quinoxalinone core were similar compounds to **14a–b**, and therefore prepared by the same synthetic way (Scheme 3).

3. Results and discussion

Our recent work regarding effective quinoxalinone-based ARIs indicated that the size of substituent groups attached to the C3 position might have an impact on the efficiency of ARIs [19]. The present study focuses on the installation of various substituent groups to quinoxalinone core structure and the activity evaluation of the resulting compounds on ALR2. The synthetic work led to

three series of compounds including *p*-nitrobenzyl derivatives (**7a–d** and **8a–d**), N1-acetate derivatives (**14a–d** and **15a–b**), and C6- or C7-substituted N1-acetate derivatives (**12**, **17**, **22**, and **23**) as shown in Table 1. All of the newly synthesized quinoxalinone derivatives were evaluated for their potential inhibitory effect on ALR2 isolated from rat lenses. The IC_{50} values were determined by linear regression analysis of log of the concentration–response curve [19–22].

Initially, compounds **7a–d** and **8a–d** series containing *p*-nitrobenzyl group on the N1 position and various bulky lipophilic moieties at the C3 position were prepared but all of them just showed a moderate ALR2 inhibition. The *p*-nitrobenzyl group seemed not suitable for the N1 position during the building of ALR2 inhibitors based on the quinoxalinone framework whereas the N1-acetate substituent was still likely to be a favored strategy [19–22]. Then, we attached nitro group at the C6 position of quinoxalinone and this resulted in the preparation of N1-acetate derivatives **12** and **17**. Both the C6-nitro substituted compounds showed significant inhibitory activity. Based on comparison, compound **12** that had a C6-nitro group and an IC_{50} value of $0.283 \mu\text{M}$ showed seven-fold more potency than its counterpart, which lacked the C6- NO_2 group reported in our previous work [19]. Also, compound **17** was about four times higher potent than compound **14b** that has no substituent at the phenyl ring of the quinoxalinone framework. Further, replacement of the C6- NO_2 group of **17** with chloro group led to compound **22**, in which the inhibition was reduced to half of **17** but was still much stronger than that of **14b**. In addition, attachment of chloro to the C7 position forming compound **23** resulted in a significantly deactivated effect when comparing the difference between **23** and **14a**. These results suggest a large impact of the N1-acetate and C3 substituents on biological activity, as well as, an enhancing role for the C6 nitro group.

Compounds **14a–d**, with N1-acetate group, were prepared in order to investigate the effect of C3 side chain on the ALR2 inhibition. Among them, C3 styrenyl-containing compound (**14a**) appeared to be the most active while the compound **14d** with more bulky C3 substituent was the least active. Hydrogenation reaction on the C3 vinyl linker of **14a–b** led to the corresponding C3 phenethyl compounds **15a–b**, respectively. Each of them was more potent in the ALR2 inhibition than its precursor indicating a benefit of the saturated linker over the vinyl linker for the biological activity. However, the *p*-fluoro group of the C3-side chain is likely to

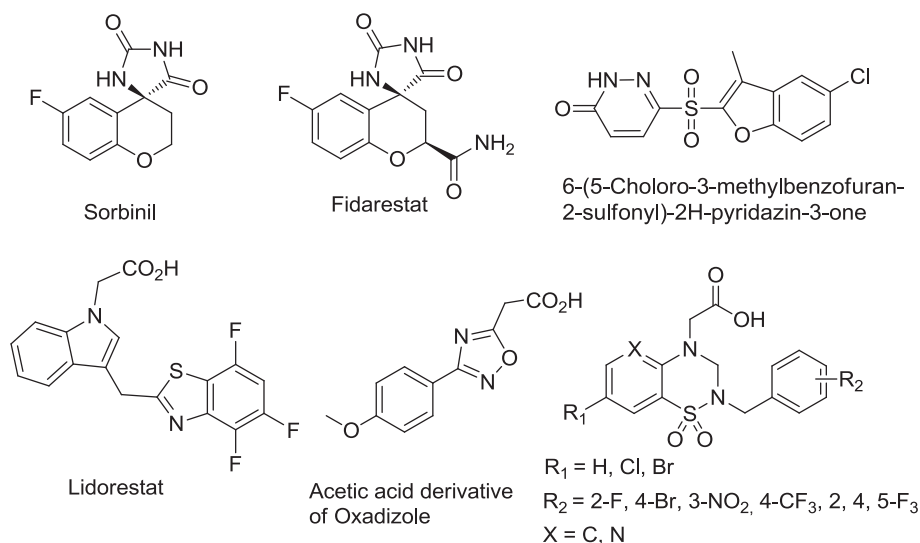
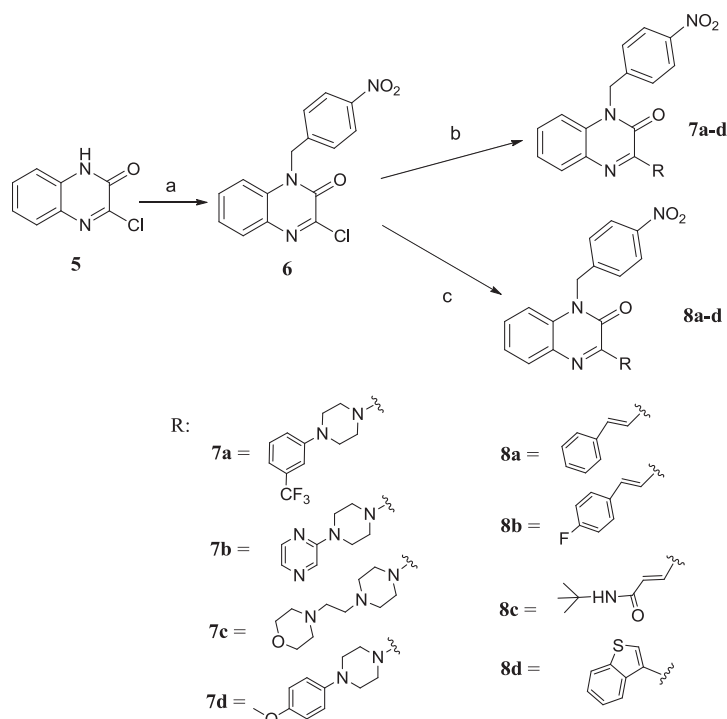


Fig. 2. Chemical structures of aldose reductase inhibitors.



Reagents and conditions: (a) 4-nitrobenzyl bromide, CH_3CN , K_2CO_3 , 12 h, N_2 , 55 °C; (b) Piperazines, DMF, K_2CO_3 , 24 h, 75 °C; (c) for the preparation of **8a–c**; Olefines, $\text{Pd}(\text{OAc})_2$, $\text{P}(\text{o-tolyl})_3$, Et_3N , DMF, 100 °C, 24 h, for **8d**; Boronic acid reagent, Cs_2CO_3 , $\text{Pd}(\text{OAc})_2$, $\text{P}(\text{Ph})_3$, N_2 , dioxane:water (30:3), 100 °C, 12 h

Scheme 1. Reagents and conditions: (a) 4-nitrobenzyl bromide, CH_3CN , K_2CO_3 , 12 h, N_2 , 55 °C; (b) Piperazines, DMF, K_2CO_3 , 24 h, 75 °C; (c) for the preparation of **8a–c**; Olefines, $\text{Pd}(\text{OAc})_2$, $\text{P}(\text{o-tolyl})_3$, Et_3N , DMF, 100 °C, 24 h, for **8d**; boronic acid reagent, Cs_2CO_3 , $\text{Pd}(\text{OAc})_2$, $\text{P}(\text{Ph})_3$, N_2 , dioxane:water (30:3), 100 °C, 12 h.

decrease the inhibitory efficiency as compared to **14a** with **14b**, and **15a** with **15b** (Table 1). The compounds, proven to be effective in ALR2 inhibition were also tested for their ability to inhibit ALR1 (aldehyde reductase) isolated from rat kidney. ALR1 is present in all tissues and plays an important role in detoxification, and therefore, has been commonly employed in the selectivity evaluation of ALR2 inhibitors (ARIs). Interestingly, our results show that **15a** and **17**, identified as significant ALR2 inhibitors, showed the least inhibitory effect on ALR1 suggesting their good selectivity for ALR2.

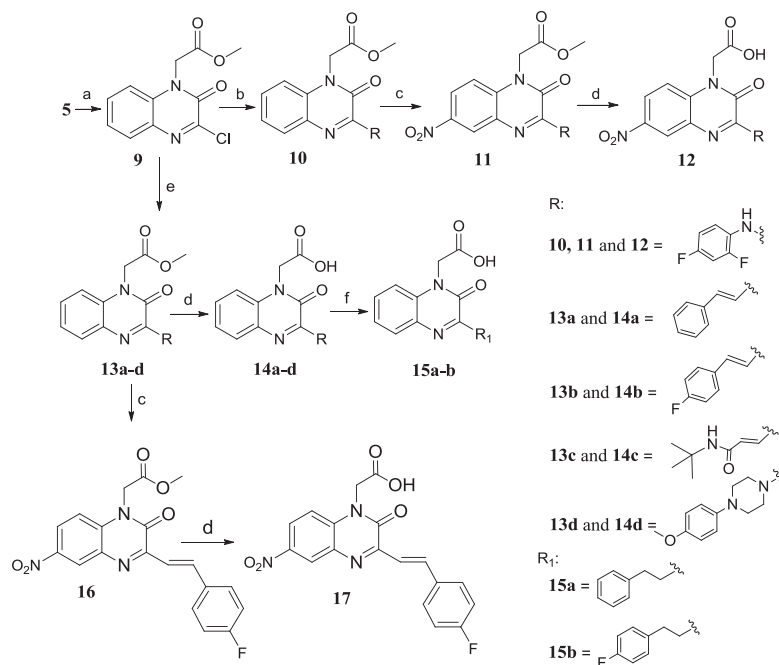
4. Molecular modeling

In order to understand the mechanistic details of biological activity and how **15a** was more active than **14a** and **17**, docking of compounds were performed with Lidorestat-bound conformation of ALR2 (PDB code: 1Z3N). As shown in Fig. 3a, b, the results of **15a** revealed that ligand fits into the active site of enzyme. The carboxylate group was fit for an anion-binding pocket through three hydrogen bonds, of which two with the hydroxyl group of Tyr 48 (3.05 Å and 3.56 Å) and one with N2 atom of His 110 (3.04 Å). The carboxyl head makes stabilizing electro-static interaction with the positive charged nicotinamide moiety of the co-factor NADP^+ ($\text{N}-\text{O} = 4.8$ Å). Additionally, the C2-carbonyl group interacts via hydrogen bonding with N1 of Trp 111 (2.39 Å) while quinoxalinone core structure penetrates into hydrophobic pocket formed by the side chains of Trp 20, Phe 122, Trp 79 and Trp 219. The C3-phenethyl ring forms a stable stacking interaction against the indol ring of Trp 111 side chain and penetrates into specificity pocket formed by Leu 300, Cys 303, Cys 298, Thr 113, Phe 122, and

Trp 111. The more flexible nature of saturated C3-linker in **15a** phenethyl group makes the compound a more favored conformation for the active site and thus stronger activity was found for **15a** over **14a**. But, in contrast, docking of **14a** (Fig. 3c–d) showed that the C2-carbonyl oxygen forms a hydrogen bond with Cys 298 (3.17 Å) and in **17** (Fig. 3e, f) showed that the C2-carbonyl oxygen forms a hydrogen bond with Cys 298 (3.11 Å), the low bond length of hydrogen bond in case of **17** was probably due to C6- NO_2 which favor the molecule to orientate slightly in to more stable way than **14a** but in both, **14b** and **17** the quinoxalinone core structures goes somewhat away from the hydrophobic pocket instead of penetrating in it as case of **15a** which indicate different interaction patterns between these compounds. The docking results provide support to **15a** as more active inhibitor.

5. Conclusion

The present effort to examine the ALR2 inhibition function of substituent groups at different positions of quinoxalinone scaffold resulted in the development of a new series of quinoxalinone ARIs including **12**, **14a–d**, **15a–b**, **17**, **22**, and **23**. They showed good to moderate activity with IC_{50} values of 0.143–7.53 μM . The most potent and selective inhibitor was found to be **15a** with N1-acetate and C3-phenethyl side chain. Besides, SAR studies suggested that the C6- NO_2 and particularly C3-phenethyl substitution were able to increase the activity. However, the substitutions at the C7 position of the scaffold and at the para-position of the phenethyl or of the C3-strenyl ring may have a decreasing effect



Reagents and conditions: (a) methyl 2-bromoacetate, CH_3CN , K_2CO_3 , 2 h, 55 °C; (b) 2,4-difluoroaniline, DMF, K_2CO_3 , 24 h, 75 °C; (c) $\text{Cu}(\text{NO}_3)_2 \cdot 3\text{H}_2\text{O}$, Ac_2O , CH_2Cl_2 , 12 h, rt; (d) LiOH , HCl ; (e) for the preparation of **13a–c**: Olefines, $\text{Pd}(\text{OAc})_2$, $\text{P}(\text{o-tolyl})_3$, Et_3N , DMF, 100 °C; for **13d**: Piperazine, Toluene, K_2CO_3 , 12 h, 100 °C; (f) Pd/C , H_2 , MeOH, 24 h, rt

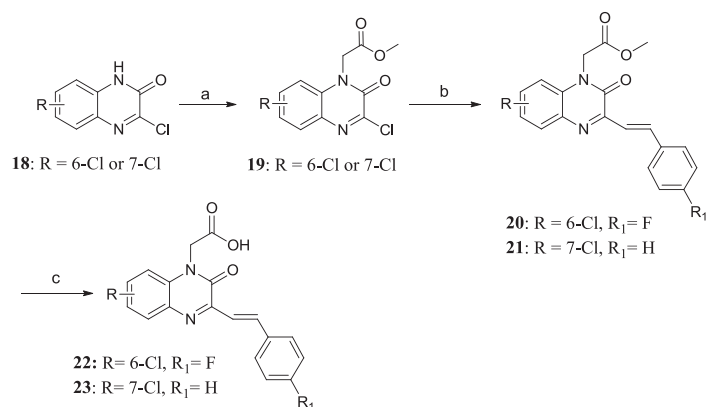
Scheme 2. Reagents and conditions: (a) methyl 2-bromoacetate, CH_3CN , K_2CO_3 , 2 h, 55 °C; (b) 2,4-difluoroaniline, DMF, K_2CO_3 , 24 h, 75 °C; (c) $\text{Cu}(\text{NO}_3)_2 \cdot 3\text{H}_2\text{O}$, Ac_2O , CH_2Cl_2 , 12 h, rt; (d) LiOH , HCl ; (e) for the preparation of **13a–c**: Olefines, $\text{Pd}(\text{OAc})_2$, $\text{P}(\text{o-tolyl})_3$, Et_3N , DMF, 100 °C; for **13d**: Piperazine, Toluene, K_2CO_3 , 12 h, 100 °C; (f) Pd/C , H_2 , MeOH, 24 h, rt.

6. Experimental section

6.1. Materials

Melting points were taken on an X-4 microscopic melting points apparatus and were uncorrected. All reactions and products mixtures purification and separation were performed by column chromatography on silica gel routinely checked by TLC on Merck_{60F254} Silica gel aluminum sheet. The purity of more potent acid derivatives was checked by HPLC. ^1H NMR and ^{13}C NMR spectra were recorded, at 400 MHz and 100 MHz in CDCl_3 and $\text{DMSO}-d_6$. Chemical shifts for

^1H NMR spectra are values from CDCl_3 (δ = 7.26 ppm). Data for ^1H NMR spectra is represented as follows: chemical shifts (ppm), multiplicity (s = singlet, d = doublet, t = triplet, q = quartet, m = multiplet), coupling constant J (Hz), and integration. ^{13}C NMR spectra data is represented in (δ = ppm). All chemicals were reagents grade. 1-(3-trifluoromethyl) phenyl piperazine, 1-(4-methoxyphenyl) piperazine, 2-(piperazin-1-yl) pyrazine, benzo[b]thiophen-3-yl boronic acid, tri-*o*-tolyl phosphine, and palladium acetate were purchased from Alfa Aesar. D,L-glyceraldehydes and NADPH were purchased from Sigma–Aldrich. Wistar rats (250–300 g) were supplied by Vital River, Beijing, China.



Scheme 3. Reagents and conditions: (a) methyl 2-bromoacetate, CH_3CN , K_2CO_3 , 2 h, 55 °C; (b) Olefines, $\text{Pd}(\text{OAc})_2$, $\text{P}(\text{o-tolyl})_3$, Et_3N , DMF, 100 °C; (c) LiOH , HCl .

Table 1 (continued)

Comp. no.	R ₁	R ₂	ALR2 inh. [%] ^a	ALR2 IC ₅₀ [μM] ^b	ALR1 inh. [%] ^a
14d		H		7.53 (6.93–8.13)	48%
15a		H		0.143 (0.125–0.161)	22%
15b		H		1.14 (1.05–1.23)	40%
22		6-Cl		0.66 (0.51–0.81)	25%
23		7-Cl		3.88 (2.90–4.86)	35%
17		6-NO ₂		0.362 (0.314–4.10)	25%
12		6-NO ₂		0.283 (0.190–3.36)	41%
Epalrestat				0.12 (0.07–0.17)	

^a Represents the percent inhibition of compounds determined at concentration of 10 μM.

^b IC₅₀ (95% CL) values represent the concentration required to effect 50% enzyme inhibition.

6.2. Synthesis of 3-chloro-1-(4-nitrobenzyl)-1, 2-dihydroquinoxaline (6)

A mixture of compound **5** (3.600 g, 20 mmol), phenols (22 mmol), DMF (10 mL) and K₂CO₃ (8.340 g, 60 mmol) was charged in 250 mL flask and refluxed at 75 °C. After 12 h the resulting mixture was cooled down and filtered. After evaporating the solvent, residue was purified by column chromatography using silica gel eluted with ethyl acetate (EtOAc)/petroleum ether (P.E) = 1:4 to furnish compound **6**. Yellow powder, yield 40%; mp: 90 °C; ¹H NMR (CDCl₃, 400 MHz) δ: 8.19 (d, *J* = 8 Hz, 2H), 7.85 (dd, *J* = 9.2, 1.1 Hz, 2H), 7.37–7.54 (m, 4H), 5.67 (s, 2H).

6.3. General procedure for the synthesis of (7a–d)

A mixture of compound **6** (150 mg, 0.5 mmol), K₂CO₃ (139 mg, 1 mmol), and appropriate piperazine and pyrazine (0.5 mmol) was charged in 250 mL flask and refluxed in 5 mL CH₃CN under argon for 4 h. Then the resulting mixture was poured into H₂O providing yellowish precipitate, which was then filtered. The residue was purified by column chromatography using silica gel eluted with EtOAc/P.E = 1:4–1:3 to afford desired products **7a–c** and **7d**.

6.3.1. 1-(4-Nitrobenzyl)-3-(4-(3-(trifluoromethyl) phenyl) piperazin-1-yl) quinoxalin-2(1H)-one (7a)

Orange powder; yield: 88%; mp: 88–90 °C; ¹H NMR (CDCl₃, 400 MHz) δ: 8.14–8.19 (m, 4H), 7.01–7.63 (m, 8H), 5.57 (s, 2H), 4.18

(s, 4H), 3.41 (s, 4H), ¹³C NMR (CDCl₃, 100 MHz) δ: 152.30, 151.37, 150.46, 147.51, 143.05, 137.8, 133.3, 132.95, 131.71, 129.76, 127.68, 125.74, 124.29, 122.91, 121.99, 116.32, 113.62, 112.42, 109.86, 48.86, 46.81, 45.77; ESI-MS([M+H]⁺) *m/z*: 510.0.

6.3.2. 1-(4-Nitrobenzyl)-3-(4-(pyrazin-2-yl) piperazin-1-yl) quinoxalin-2(1H)-one (7b)

Dark yellow powder; yield: 85%; mp: 220–222 °C; ¹H NMR (CDCl₃, 400 MHz) δ: 8.10–8.19 (m, 3H), 7.38 (d, *J* = 8 Hz, 2H), 7.01–7.63 (m, 8H), 5.57 (s, 2H, –CH₂–), 4.09–4.15 (m, 4H), 3.77–3.79 (m, 4H), ¹³C NMR (CDCl₃, 100 MHz) δ: 152.0, 152.34, 150.53, 147.56, 143.02, 141.92, 133.52, 131.13, 129.81, 127.45, 125.83, 124.33, 113.65, 109.90, 46.63, 45.82, 44.50; ESI-MS([M+H]⁺) *m/z*: 444.3.

6.3.3. 1-(4-Nitrobenzyl)-3-(4-(2-morpholinoethyl) piperazin-1-yl) quinoxalin-2(1H)-one (7c)

Yellow powder; yield: 85%; mp: 210–212 °C; ¹H NMR (CDCl₃, 400 MHz) δ: 8.01 (d, *J* = 8.4 Hz, 2H), 6.8–7.43 (m, 6H), 5.39 (s, 2H), 3.85 (s, 4H), 3.56 (s, 4H), 2.36–2.52 (m, 12H), ¹³C NMR (CDCl₃, 100 MHz) δ: 152.26, 150.51, 147.42, 134.31, 133.50, 129.64, 127.63, 127.18, 125.33, 124.20, 113.50, 67.02, 56.45, 55.75, 54.24, 53.77, 46.98, 45.70; ESI-MS([M+H]⁺) *m/z*: 479.1.

6.3.4. 1-(4-Nitrobenzyl)-3-(4-(4-methoxyphenyl) piperazin-1-yl) quinoxalin-2(1H)-one (7d)

Yellow powder; yield: 70%; mp: 220–225 °C; ¹H NMR (CDCl₃, 400 MHz) δ: 9.1 (s, 1H), 8.15 (d, *J* = 8.4 Hz, 2H), 6.83–7.5 (m, 9H),

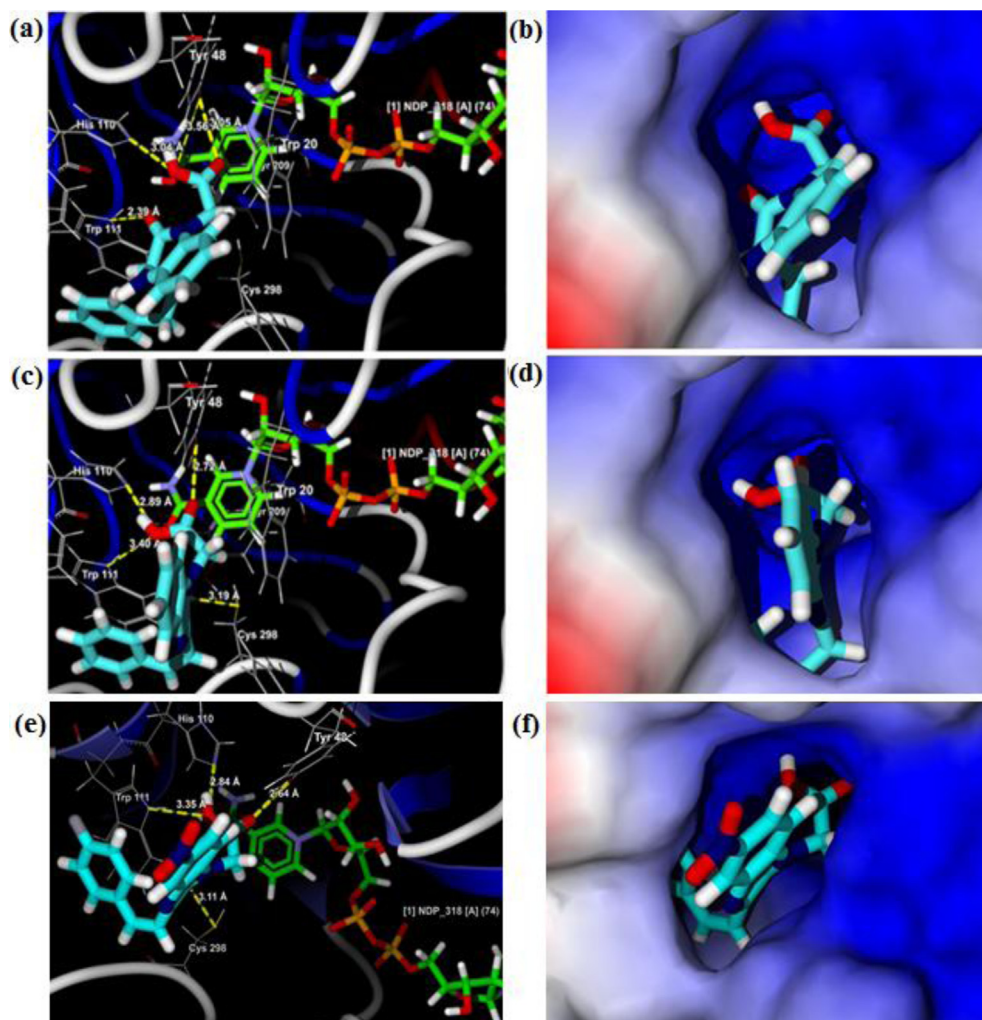


Fig. 3. Docking of inhibitors in to active site of ALR2. a) Docking of **15a** in to ALR2 active site in ribbon diagram; b) in surface representation. The docked pose of **15a** shown in cyan (C), blue (N) and red (O); hydrogen bonds are shown as light yellow dashed lines; c) Docking of **14a** in to ALR2 active site in ribbon diagram; d) in surface representation. The docked pose of **14a** shown in cyan (C), blue (N) and red (O); hydrogen bonds are shown as light yellow dashed lines; e) Docking of **17** in to ALR2 active site in ribbon diagram; f) in surface representation. The docked pose of **17** shown in cyan (C), blue (N) and red (O); hydrogen bonds are shown as light yellow dashed lines.

5.54 (s, 2H), 4.1 (s, 4H), 3.2 (m, 4H), 3.7 (s, 3H), ^{13}C NMR (CDCl_3 , 100 MHz) δ : 150.60, 145.64, 143.10, 129.76, 127.68, 127.32, 125.56, 124.44, 118.62, 114.58, 113.58, 55.67, 50.99, 47.18, 45.76; ESI-MS($[\text{M}+\text{H}]^+$) m/z : 472.1.

6.4. General procedure for the synthesis of **8a–c**

A mixture of compound **6** (315 mg, 1 mmol), appropriate olefinic reagent (1.5 mmol), palladium acetate (0.3 mmol), tri-*o*-tolyl phosphine (0.7 mmol) and triethylamine (2 mmol) in DMF (5 mL) was refluxed for 24 h, and then poured into water and filtered. The residue was purified by column chromatography eluted with EtOAc/P.E = 1:4 to afford products **8a–c**.

6.4.1. 1-(4-Nitrobenzyl)-3-styrylquinoxalin-2(1H)-one (**8a**)

Orange solid; yield: 60%; mp: 200–205 °C; ^1H NMR (CDCl_3 , 400 MHz) δ : 8.16–8.21 (m, 3H), 7.69 (d, J = 8 Hz, 2H, aromatic), 7.77 (d, J = 16 Hz, 2H), 7.40–7.44 (m, 6H), 7.10 (d, J = 8 Hz, 2H), 5.63 (s, 2H), ^{13}C NMR (CDCl_3 , 100 MHz) δ : 155.11, 152.65, 147.61, 138.88, 136.34, 133.81, 131.95, 130.10, 129.61, 129, 128.1, 127.82, 124.38, 121.86, 113.90, 45.63; ESI-MS($[\text{M}+\text{H}]^+$) m/z : 384.3.

6.4.2. 3-(4-Fluorostyryl)-1-(4-nitrobenzyl) quinoxalin-2(1H) – one (**8b**)

Orange solid; yield: 60%; mp: 200–202 °C; ^1H NMR (CDCl_3 , 400 MHz) δ : 8.12 (dd, J = 22, 12.4 Hz, 2H), 7.90 (d, J = 8 Hz, 2H), 7.0–7.71 (m, 10H), 5.63 (s, 2H), ^{13}C NMR (CDCl_3 , 100 MHz) δ : 155.10, 152.55, 147.60, 137.54, 130.47, 130.15, 129.87, 127.81, 124.55, 121.86, 124.36, 121.62, 116.16, 115.94, 113.92, 45.62; ESI-MS($[\text{M}+\text{H}]^+$) m/z : 402.3.

6.4.3. N-(Tert-butyl)-3-(4-(4-nitrobenzyl)-3-oxo-3, 4-dihydroquinoxalin-2-yl) acryl amide (**8c**)

Pale yellow solid; yield: 60%; mp: 210 °C; ^1H NMR (CDCl_3 , 400 MHz) δ : 8.18 (d, J = 8 Hz, 2H), 7.90 (dd, J = 12.2, 6.1 Hz, 2H), 7.26–7.48 (m, 4H), 7.11 (d, J = 8 Hz, 2H), 5.63 (s, 2H), 1.45 (s, 9H), ^{13}C NMR (CDCl_3 , 100 MHz) δ : 164.44, 154.71, 151.30, 147.64, 142.54, 133.68, 133.54, 132.41, 131.46, 131.23, 127.82, 124.62, 113.97, 109.90, 51.85, 45.58, 28.88; ESI-MS($[\text{M}+\text{H}]^+$) m/z : 407.4.

6.5. Synthesis of 3-(Benzo[*b*] thiophen-3-yl)-1-(4-nitrobenzyl) quinoxalin-2(1H)-one (**8d**)

A mixture of compound **6** (315 mg, 1 mmol), appropriate boronic acid reagent (196 mg, 1.1 mmol), palladium acetate (5 mg,

0.05 mmol), triphenyl phosphine (20 mg, 0.015 mmol) and Cesium carbonate (650 mg, 2 mmol) in solution of dioxane:water (30:3) was refluxed under inert atmosphere at 100 °C for 12 h and monitored by TLC, then washed the mixture with aqueous sodium chloride solution and extracted with THF. Dried the organic layer with MgSO_4 , and filtered off. After evaporating the solvent in vacuo, the residue was purified by column chromatography using silica gel eluted EtOAc/PE = 1:3 to afford **8d**. Pale yellow solid; yield: 70%; mp: 195–200 °C; ^1H NMR (CDCl_3 , 400 MHz) δ : 8.88 (s, 1H), 7.15–8.19 (m, 12H), 5.69 (s, 2H), ^{13}C NMR (CDCl_3 , 100 MHz) δ : 153.25, 148.16, 151.30, 147.28, 142.32, 141.57, 140.18, 140.07, 133.04, 132.73, 131.51, 130.35, 127.49, 126.19, 125.16, 124.27, 122.75, 113.54, 45.58; ESI-MS($[\text{M}+\text{H}]^+$) m/z : 415.4.

6.6. Compounds **9** and **10**

Procedure and data reported previously [19].

6.7. Synthesis of 2-(3-(2,4-difluorophenylamino)-6-nitro-2-oxoquinoxalin-1(2H)-yl) acetic acid methyl ester **11**

A solution of $\text{Cu}(\text{NO}_3)_2 \cdot 3\text{H}_2\text{O}$ (223 mg, 1 mmol) in acetic anhydride (10 mL) was stirred for 2 h at room temperature, and then a solution of compound **10** (173 mg, 0.5 mmol) [21] in CH_2Cl_2 (10 mL) was added in it. The reaction solution was stirred for 12 h at room temperature. After it, MeOH (10 mL) added to the resulting solution and the stirring was continued until the mixture becomes clear solution. Solvent was evaporated, and the residue was neutralized with aqueous solution of NaHCO_3 to pH 6. The precipitate was collected by filtration, washed with water and purified with column chromatography eluted with EtOAc/PE = 1:3 to furnish the product **11**. Yellow powder; yield: 55%; mp: 225 °C; ^1H NMR (CDCl_3 , 400 MHz) δ : 10.48 (s, 1H), 8.34 (s, 1H), 7.85 (d, J = 8.9 Hz, 1H), 8.19 (m, 4H), 5.63 (s, 2H), 3.74 (s, 3H).

6.8. Synthesis of 2-(3-(2,4-difluorophenylamino)-6-nitro-2-oxoquinoxalin-1(2H)-yl) acetic acid (**12**)

To a solution of ester **11** (195 mg, 0.5 mmol) in THF (5 mL) was added saturated aqueous LiOH (5 mL). The mixture was stirred at room temperature for 2 h, and then acidified to pH 1–2. The precipitate was filtered off and washed with water to afford the product. Yellow powder; yield: 70%; mp: 290 °C; ^1H NMR (400 MHz, $\text{DMSO}-d_6$) δ : 10.31 (s, 1H), 7.71–8.17 (m, 5H), 7.68 (d, J = 4 Hz, 1H), 5.1 (s, 2H), ^{13}C NMR (100 MHz, $\text{DMSO}-d_6$) δ : 169.94, 151.47, 151.20, 149.10, 147.97, 144.41, 137.55, 136.61, 135.42, 129.92, 119.52, 110.47, 105.65, 105.40, 19.9; ESI-MS($[\text{M}+\text{H}]^+$) m/z : 377.1; HRMS (ESI) m/z calcd for $[\text{M}-\text{H}]^-$ 375.0939 found 376.9744.

6.9. General procedure for the synthesis of compounds **13a–c**, **16**, **19**, **20** and **21**

Same procedure as for **8a–c**.

6.9.1. 2-(2-Oxo-3-styrylquinoxalin-1(2H)-yl) acetic acid methyl ester (**13a**)

Yellow powder; yield: 70%; mp: 160 °C; ^1H NMR (CDCl_3 , 400 MHz) δ : 8.18 (d, J = 16.2 Hz, 1H), 7.91 (d, J = 7.9 Hz, 1H), 7.71 (dd, J = 19.5, 11.8 Hz, 2H), 7.50 (t, J = 7.7 Hz, 1H), 7.25–7.40 (m, 5H), 7.08 (d, J = 7.9 Hz, 1H), 5.09 (s, 2H), 3.8 (s, 3H).

6.9.2. 2-(3-(4-Fluorostyryl)-2-oxoquinoxalin-1(2H)-yl) acetic acid methyl ester (**13b**)

Yellow powder; yield: 70%; mp: 165 °C; ^1H NMR (400 MHz, $\text{DMSO}-d_6$) δ : 8.05 (d, J = 16.2 Hz, 1H), 7.61 (dd, J = 19.5, 11.8 Hz, 2H), 7.25–7.40 (m, 6H), 7.08 (d, J = 7.9 Hz, 1H), 5.2 (s, 2H), 3.4 (s, 3H).

6.9.3. Methyl 2-(3-(3-(tert-butylamino)-3-oxoprop-1-en-1-yl)-2-oxoquinoxalin-1(2H)-yl) acetate (**13c**)

Synthesized and used immediately for next step to prepare **14c**.

6.9.4. 2-(3-(4-Fluorostyryl)-6-nitro-2-oxoquinoxalin-1(2H)-yl) acetic acid methyl ester (**16**)

Orange powder; Yield: 70%; mp: 130 °C; ^1H NMR (400 MHz, $\text{DMSO}-d_6$) δ : 8.90 (s, 1H), (d, J = 8 Hz, 1H), 7.22–7.60 (m, 7H), 5.17 (s, 2H), 3.6 (s, 3H).

6.9.5. Compound **19**

Procedure and data reported previously [19].

6.9.6. 2-(6-Chloro-2-oxo-3-styrylquinoxalin-1(2H)-yl) acetic acid methyl ester (**20**)

Synthesized and used immediately for next step to prepare **22**.

6.9.7. 2-(7-Chloro-2-oxo-3-styrylquinoxalin-1(2H)-yl) acetic acid methyl ester (**21**)

Yellow powder; yield: 45%; mp: 180 °C; ^1H NMR (CDCl_3 , 400 MHz) δ : 7.60 (d, J = 8 Hz, 2H), 7.59 (s, 1H), 7.18–7.36 (m, 6H), 6.90 (d, J = 12 Hz, 1H), 4.96 (s, 2H), 3.6 (s, 3H).

6.10. Synthesis of methyl 2-(3-(4-(4-methoxyphenyl) piperazin-1-yl)-2-oxoquinoxalin-1(2H)-yl) acetate (**13d**)

A mixture of compound **9** (252 mg, 1 mmol), K_2CO_3 (278 mg, 2 mmol), and 1-(4-methoxyphenyl) piperazine (192 mg, 1 mmol) was charged in 100 mL flask and refluxed in 10 mL Toluene under argon for 12 h. After evaporating the solvent, the residue was purified by column chromatography using silica gel eluted with EtOAc/PE = 1:3 to get desired product. Off-white powder; yield: 70%; mp: 185–190 °C; ^1H NMR (400 MHz, $\text{DMSO}-d_6$) δ : 6.08–7.27 (m, 8H), 5.08 (s, 2H), 4.09 (s, 4H), 3.67 (s, 4H), 2.59 (s, 6H).

6.11. Synthesis of **14a–d**, **17**, **22**, and **23**

Same procedure as for **12**.

6.11.1. 2-(2-Oxo-3-styrylquinoxalin-1(2H)-yl) acetic acid (**14a**)

Yellow powder; yield: 70%; mp: 215 °C; ^1H NMR (400 MHz, $\text{DMSO}-d_6$) δ : 8.05 (d, J = 16.2 Hz, 1H), 7.4–7.8 (m, 10H), 5.07 (s, 2H), ^{13}C NMR (100 MHz, $\text{DMSO}-d_6$) δ : 168.78, 154.09, 151.43, 137.55, 135.83, 132.62, 130.35, 129.58, 129.41, 129.07, 127.77, 124.04, 112.83, 114.60, 53.0; ESI-MS($[\text{M}-\text{H}]^-$) m/z : 305.1; HRMS (ESI) m/z calcd for $[\text{M}-\text{H}]^-$ 305.095 found 305.0943.

6.11.2. 2-(3-(4-Fluorostyryl)-2-oxoquinoxalin-1(2H)-yl) acetic acid (**14b**)

Yellow powder, yield: 70% mp: 215 °C; ^1H NMR (400 MHz, $\text{DMSO}-d_6$) δ : 8.07 (d, J = 16.3 Hz, 1H), 7.84 (dd, J = 16.8, 8.2 Hz, 1H), 7.53 (m, 6H), 7.41 (t, J = 7.5 Hz, 1H), 7.28 (t, J = 8.8 Hz, 1H) 5.09 (s, 2H), ^{13}C NMR (100 MHz, $\text{DMSO}-d_6$) δ : 168.83, 164, 161.54, 151.38, 136.31, 132.60, 132.51, 132.28, 130.32, 130, 129.92, 129.38, 124, 121.74, 116.11, 115.90, 114.61, 53.8; ESI-MS($[\text{M}-\text{H}]^-$) m/z : 323.1; HRMS (ESI) m/z calcd for $[\text{M}-\text{H}]^-$ 323.0837 found 323.0836.

6.11.3. 2-(3-(3-(Tert-butylamino)-3-oxoprop-1-en-1-yl)-2-oxoquinoxalin-1(2H)-yl) acetic acid (**14c**)

Brown powder; yield: 50%; mp: 115 °C; ¹H NMR (400 MHz, DMSO-*d*₆) δ: 7.83 (s, 1H), 7.46–7.81 (m, 3H), 7.43 (d, *J* = 12 Hz, 1H), 7.39 (d, *J* = 8 Hz, 1H), 5.00 (s, 2H), 1.29 (s, 9H), ¹³C NMR (100 MHz, DMSO-*d*₆) δ: 171.11, 169.71, 169.22, 164.14, 154.37, 151.12, 133.20, 132.82, 132.60, 132.31, 132.12, 131.99, 131.95, 131.80, 130.24, 129.10, 124.59, 115.18, 67.49, 65.53, 30.28, 28.89, 28.84, 25.55; ESI-MS([M+H]⁺) *m/z*: 330.3.

6.11.4. 2-(3-(4-(4-Methoxyphenyl) piperazin-1-yl)-2-oxoquinoxalin-1(2H)-yl) acetic acid (**14d**)

Off-white powder; yield: 50%; mp: 200 °C; ¹H NMR (400 MHz, DMSO-*d*₆) δ: 6.85–7.51 (m, 8H), 4.98 (s, 2H), 4.04 (s, 4H), 3.69 (s, 3H), 3.19 (s, 4H), ¹³C NMR (100 MHz, DMSO-*d*₆) δ: 168.95, 151.39, 149.98, 132.36, 130.11, 126.20, 125.31, 123.72, 114.35, 114.01, 55.26, 50.13, 46.13, 43.93, 39.72, 39.25; HRMS (ESI) *m/z* calcd for [M-H]⁻ 393.1568 found 393.1581.

6.11.5. 2-(3-(4-Fluorostyryl)-6-nitro-2-oxoquinoxalin-1(2H)-yl) acetic acid (**17**)

Orange powder; yield: 45%; mp: 190 °C; ¹H NMR (400 MHz, DMSO-*d*₆) δ: 8.64 (s, 1H), 7.31–7.95 (m, 7H), 7.27 (d, *J* = 8 Hz, 1H), 5.28 (s, 2H), ¹³C NMR (100 MHz, DMSO-*d*₆) δ: 168.06, 142.94, 138.01, 134.30, 133.57, 133.50, 132.66, 132.55, 130.97, 130.25, 129.1, 126.36, 126.24, 125.18, 116.97, 116.76, 115.63, 65.51; ESI-MS([M+H]⁺) *m/z*: 372.3; HRMS (ESI) *m/z* calcd for [M+H]⁺ 372.3018 found 372.0939.

6.11.6. 2-(6-Chloro-3-(4-fluorostyryl)-2-oxoquinoxalin-1(2H)-yl) acetic acid (**22**)

Yellow powder; yield: 45%; mp: 280 °C; ¹H NMR (400 MHz, DMSO-*d*₆) δ: 7.63 (d, *J* = 12 Hz, 1H), 7.51–7.42 (m, 4H), 7.40 (d, *J* = 8 Hz, 1H), 7.23–7.39 (m, 3H), 5.00 (s, 2H), ¹³C NMR (100 MHz, DMSO-*d*₆) δ: 196.17, 164.51, 162.04, 154.32, 152.02, 137.23, 135.16, 133.82, 132.83, 132.80, 130.51, 130.42, 124.59, 121.94, 116.57, 116.35, 114.93, 67.48; ESI-MS([M+H]⁺) *m/z*: 359.3; HRMS (ESI) *m/z* calcd for [M-H]⁻ 339.0542 found 339.056.

6.11.7. 2-(7-Chloro-2-oxo-3-styrylquinoxalin-1(2H)-yl) acetic acid (**23**)

Yellow powder, yield: 35%; mp: 270 °C; ¹H NMR (400 MHz, DMSO-*d*₆) δ: 8.041 (d, *J* = 10.8, 1H), 8.02 (d, *J* = 5.2, 1H), 7.39–7.88 (m, 8H), 5.10 (s, 2H), ¹³C NMR (100 MHz, DMSO-*d*₆) δ: 169.21, 154.30, 153.26, 139.17, 138.80, 136.10, 136.01, 133.76, 133.68, 131.98, 131.62, 130.30, 129.54, 128.08, 122.07, 117.08, 116.90, 53.02; ESI-MS([M+H]⁺) *m/z*: 341.1; HRMS (ESI) *m/z* calcd for [M-H]⁻ 339.0542 found 339.0560.

6.12. General procedure of synthesis of **15a** and **15b**

To a suspension of 10% palladium over carbon (50 mg) in methanol was added a solution of appropriate compound **14a** or **14b** (0.25 mmol) in EtOAc (10 mL). The mixture was stirred at room temperature under hydrogen atmosphere for 18 h. The catalyst was filtered off through celite. The filtrate was concentrated and the residue was purified by column chromatography using CH₂Cl₂/MeOH (40:2) as eluent to obtain products as off-white powder.

6.12.1. 2-(2-Oxo-3-phenethylquinoxalin-1(2H)-yl) acetic acid (**15a**)

Off-white powder; yield: 70%; mp: 120 °C; ¹H NMR (400 MHz, DMSO-*d*₆) δ: 7.75 (d, *J* = 7.9 Hz, 1H), 7.49 (t, *J* = 10.1 Hz, 1H), 7.17–7.32 (m, 7H), 4.70 (s, 2H), 3.01–3.11 (m, 4H), ¹³C NMR (100 MHz, DMSO-*d*₆) δ: 159.68, 154.27, 141.99, 133.30, 132.31, 130.01, 129.28, 128.85, 128.79, 126.35, 123.55, 115.43, 53.0, 35.66, 32.12; ESI-

MS([M-H]⁻) *m/z*: 307.3; HRMS (ESI) *m/z* calcd for [M-H]⁻ 307.1088 found 307.1070.

6.12.2. 2-(3-(4-Fluorophenethyl)-2-oxoquinoxalin-1(2H)-yl) acetic acid (**15b**)

Off-white powder; yield: 70%; mp: 130 °C; ¹H NMR (400 MHz, DMSO-*d*₆) δ: 7.75 (dd, *J* = 7.9, 1.3 Hz, 1H), 7.06–7.50 (m, 8H), 4.68 (s, 2H), 3.01–3.12 (m, 4H), ¹³C NMR (100 MHz, DMSO-*d*₆) δ: 160.31, 158.37, 154.12, 140.99, 132.24, 132.35, 129.09, 128.41, 129.11, 125.55, 123.45, 115.33, 53.0, 35.34, 32.23; ESI-MS([M-H]⁻) *m/z*: 325.3.

6.13. Biological methods

ALR2 and ALR1 were obtained from Wistar rats containing about 200–250 g body weight, supplied by Vital River, Beijing China. D,L-glyceraldehyde, Sodium D-glucuronate and NADPH were obtained from Sigma Aldrich. ALR2 and ALR1 were prepared by methods of La Motta et al. [16] and Kinoshita [25]. All chemical used were of reagent grade. Enzyme and target compounds inhibition activities were tested using Shimadzu UV-1800 Spectrophotometer by monitoring change in absorption at λ = 340 nm, resulting oxidation of NADPH by ALR2 and ALR1.

6.14. Enzymatic assay

ALR2 was prepared by methods of La Motta et al. [16] and Kinoshita [25]. The freshly acquired rat eye lenses were homogenized (Glass-potter) in three volumes of deionized water in an ice bath. The homogenate was then centrifuged for 30 min at 12,000 rpm (rotor type: 12154-H) at 0–4 °C. The supernatant was precipitated with (NH₄)₂SO₄ at 40% and at 50% saturation. The combined supernatant of both 40% and at 50% saturation then precipitated with (NH₄)₂SO₄ at 75%. The final precipitated obtained from the 75% saturated fraction, which was determined to possess ALR2 activity, was dissolved in 0.05 M NaCl and dialyzed overnight and stored at –20 °C. The dialyzed material was used for enzymatic assay.

The ALR2 activity was performed at 30 °C in a reaction mixture of 1 mL solution containing 0.25 mL NADPH (0.10 mM), 0.25 mL sodium phosphate buffer (0.1 M, pH 6.2), 0.1 mL enzyme extract, 0.15 mL deionized water and 0.25 mL D,L Glyceraldehyde (10 mM) as a substrate. The reaction mixture was incubated at 30 °C for 10 min except for D,L Glyceraldehyde. Then substrate added to start the reaction and monitored for 4 min. The ALR1 activity assay was done at 37 °C in a reaction mixture containing 0.25 mL NADPH (0.10 mM), 0.25 mL sodium phosphate buffer (0.1 M, pH 7.2), 0.1 mL enzyme extract, 0.15 mL deionized water and 0.25 mL sodium D-Glucuronate (20 mM) as a substrate in a final volume of 1 mL. The reaction mixture was incubated at 37 °C for 10 min except for sodium D-Glucuronate. After it substrate was added to start the reaction and monitored for 4 min.

The inhibitory activity of newly synthesized compounds against ALR2 and ALR1 were assayed by adding 5 μL inhibitor solution to the above mentioned reaction mixture. All compounds were dissolved in DMSO and diluted with deionized water. To correct for non-enzymatic oxidation of NADPH, the rate of NADPH oxidation in the presence of all of the reaction mixture components except the substrate was subtracted from each experimental rate. The inhibitory effect of synthetic compounds was routinely estimated at concentration of 10⁻⁵ M (The concentration is referenced to that of compounds in the reaction mixture). The active compounds were tested at an additional concentration between 10⁻⁶ and 10⁻⁷ M. Each dose effect curve was generated with at least three concentrations of inhibitors between 20 and 80%, with three replicates at each concentration.

6.15. Molecular docking

Docking studies were performed using Molegro Virtual Docker, version 5.0. The crystal structure of the human aldose reductase with bound inhibitor (PDB code: 1Z3N) retrieved from the RCSB Protein Data Bank [10] and used for docking. Water and other solvents within the protein structure were removed for docking procedure. All the structural parameters of the ligands such as bond order, hybridization, explicit hydrogen atoms and charges were assigned when necessary in the Molegro Virtual Docker software. For the better potential, binding sites in protein, and five binding cavities were selected, the cavity around the anion binding site (volume of $\sim 124 \text{ \AA}^3$) was chosen for the docking calculations. All docking calculations were carried out using the grid-based MolDock score (GRID) function with a grid resolution of 0.30 \AA . From the MolDock score and ReRank score best ligand poses were chosen.

Acknowledgments

This work was supported by the National Natural Science Foundation of China (grant no. 21272025), the Research Fund for the Doctoral Program of Higher Education of China (grant no. 20111101110042), and the Science and Technology Commission of Beijing (China) (grant no. Z131100004013003).

Appendix A. Supplementary data

Supplementary data related to this article can be found at <http://dx.doi.org/10.1016/j.ejmech.2014.04.047>.

References

- [1] P. Alexiou, K. Pegklidou, M. Chatzopoulou, I. Nicolaou, V.J. Demopoulos, *Current Medicinal Chemistry* 16 (2009) 734–752.
- [2] C. Yabe-Nishimura, *Pharmacological Reviews* 50 (1998) 21–33.
- [3] S.M. Chung, S.K. Chung, *Current Medicinal Chemistry* 10 (2003) 1375–1387.

- [4] Y.L. Kao, K. Donaghue, A. Chan, J. Knight, M. Silink, *Diabetes* 48 (1999) 1338–1340.
- [5] D.K. Moczulski, W. Burak, A. Doria, M. Zychma, E. Zukow-ska-Szczechowska, J.H. Warram, W. Grzeszczak, *Diabetologia* 42 (1999) 94–97.
- [6] V.F. Carvalho, E.O. Barreto, M.F. Serra, R.S. Cordeiro, M.A. Maritus, Z.B. Fortes, P.M. e Silva, *European Journal of Pharmacology* 549 (2006) 173–178.
- [7] R. Kikkawa, I. Hatanaka, H. Yasuda, N. Kobayashi, Y. Shigeta, H. Tarashima, T. Morimua, M. Tsuboshima, *Diabetologia* 24 (1983) 290–292.
- [8] M.A. Ramirez, N.L. Borja, *Pharmacotherapy* 28 (2008) 646–655.
- [9] S. Ao, Y. Shingu, C. Kikuchi, Y. Takano, K. Nomura, T. Fujiwara, Y. Ohkubo, Y. Notsu, I. Yamaguchi, *Metabolism* 40 (1991) 77–87.
- [10] M.C. Van Zandt, M.L. Jones, D.E. Gunn, L.S. Geraci, J.H. Jones, D.R. Sawicki, J. Sredy, J.L. Jacot, A.T. DiCioccio, T. Petrova, A. Mitschler, A.D. Podjarny, *Journal of Medicinal Chemistry* 48 (2005) 3141–3152.
- [11] C. La Motta, S. Sartini, S. Salerno, F. Si-morini, S. Taliani, A.M. Marini, F. Da Settimo, L. Marinelli, V. Limongelli, E. Novellino, *Journal of Medicinal Chemistry* 51 (2008) 3182–3193.
- [12] W.G. Robison Jr., N.M. Laver, J.L. Jacot, J.P. Glover, *Investigative Ophthalmology & Visual Science* 36 (1995) 2368–2380.
- [13] T. Asano, Y. Saito, M. Kawakami, N. Yamada, *Journal of Diabetes and its Complication* 16 (2002) 133–138.
- [14] T. Negoro, M. Murata, S. Ueda, B. Fujitani, Y. Ono, A. Kuromiya, M. Komiya, K. Suzuki, J.-i. Matsumoto, *Journal of Medicinal Chemistry* 41 (1998) 4118–4129.
- [15] B.L. Mylari, S.J. Armento, D.A. Beebe, E.L. Conn, J.B. Coutcher, M.S. Dina, M.T. O’Gorman, M.C. Linhares, W.H. Martin, P.J. Oates, D.A. Tess, G.J. Withbroe, W.J. Zembrowski, *Journal of Medicinal Chemistry* 48 (2005) 6326–6339.
- [16] C. La Motta, S. Sartini, L. Mugnaini, F. Simorini, S. Taliani, S. Salerno, A.M. Marini, F. Da Settimo, A. Lavecchia, E. Novellino, M. Can-tore, P. Failli, M. Ciuffi, *Journal of Medicinal Chemistry* 50 (2007) 4917–4927.
- [17] P. Alexiou, V.J. Demopoulos, *Journal of Medicinal Chemistry* 53 (2010) 7756–7766.
- [18] S.R. Sharma, N. Sharma, *Annals of Indian Academy of Neurology* 11 (2008) 231–235.
- [19] Y. Yang, S. Zhang, B. Wu, X. Chen, X. Qin, M. He, S. Hussain, C. Jing, B. Ma, C. Zhu, *Chemistry Medicinal Chemistry* 7 (2012) 823–835.
- [20] X. Chen, S. Zhang, Y. Yang, S. Hussain, M. He, D. Gui, B. Ma, C. Jing, Z. Qiao, C. Zhu, Q. Yu, *Bioorganic & Medicinal Chemistry* 19 (2011) 7262–7269.
- [21] X. Chen, Y. Yang, B. Ma, S. Zhang, M. He, D. Gui, S. Hussain, C. Jing, C. Zhu, Q. Yu, Y. Liu, *European Journal of Medicinal Chemistry* 46 (2011) 1536–1544.
- [22] X. Chen, C. Zhu, F. Guo, X. Qiu, Y. Yang, S. Zhang, M. He, S. Parveen, C. Jing, Y. Li, B. Ma, *Journal of Medicinal Chemistry* 53 (2010) 8330–8344.
- [23] M. Azaam, W.M. De Borggraeve, F. Compennolle, G.J. Hoornaert, *Tetrahedron* 61 (2005) 3953–3962.
- [24] P. Romea, M. Aragones, J. Garcia, J. Vilarrasa, *Organic Letters* 56 (1991) 7038–7042.
- [25] S. Hayman, J.H. Kinoshita, *Journal of Biological Chemistry* 240 (1965) 877–882.